have a strong tendency to become smaller than the values required for the planar structures. The lowest value (3500 cm^{-1} or 10.0 kcal/mol) of B_{pt} occurs, however, for the dioxin molecule with no CH_2–CH_2 torsional interactions. Among these molecules the barrier to interconversion (B_{int}), which is the energy between the twisted and bent forms, was calcualted to be between 3120 and 3600 cm^{-1}, and these values correspond to energy differences between planar and bent forms of 150 to 1100 cm^{-1}. The lowest of these B_{pb} values is for thiopyran, the highest for cyclohexene.

Comparison to Previous Studies. As discussed above, the previous infrared and Raman studies of DCC and SW did not utilize two-dimensional potential energy functions to simultaneously analyze their ring-twisting and ring-bending data. Thus, their approximations, which resulted in much larger energy differences between the planar and twisted energy structures (B_{pt}) and between planar and bent forms ($B_{pb} = B_{pt} - B_{int}$), cannot be considered to be reliable.

On the other hand, the twist angle of 30.1° reported from microwave work[4] is in reasonably good agreement with our value of 39.0°. Since both the ring-twisting and ring-bending are large-amplitude vibrations, the molecule distorts considerably even in the vibrational ground state during the course of its out-of-plane vibrations.

The nuclear magnetic resonance studies of cyclohexene[3] and its analogues[17-19] in solution have resulted in calculated barriers to interconversion which are 600–1800 cm^{-1} less than those calculated from our infrared data. Differences are expected in as much as the NMR work was carried out in vinyl chloride or Freon-21 as solvents rather than in the gas phase. Nonetheless, the 1780-cm^{-1} difference in B_{int} for cyclohexene is surprising. Our data could still be fit reasonably well using a B_{int} value as low as 3200 cm^{-1} (instead of 3600 cm^{-1}), but in this case a new pair of minima occur in the potential energy surface corresponding to bent forms (i.e. one form is bent "up" and one bent "down"). We do not believe such minima exist. Our data clearly do show that B_{int} for the gas phase is much larger than the reported NMR value of 1820 cm^{-1} for the solution.

In Table VI we have also compared our results to predictions from molecular mechanics programs (MM2).[20] The MM2 parameters have been derived from existing empirical data in the literature and are intended primarily to predict structure rather than energy differences. In all cases, the molecular mechanics calculations predict both B_{pt} and B_{int} values to be less than those we have determined. Qualitatively, the relative magnitudes for B_{pt} among the six molecules are in agreement. However, B_{int} values agree less well.

In summary, the potential energy surface derived from our infrared data show the cyclohexene molecule to be twisted by 39.0°, a value considerably smaller than previously predicted from vibrational data by DCC and SW. This twist angle, however, is larger than reported in a microwave study.[6] The twist form was found to be 13.4 ± 1.4 kcal/mol lower in energy than the planar form while the bent form, which represents a saddle point on the energy surface, lies approximately 3.1 kcal/mol below the planar form and 10.3 kcal/mol above the twisting minimum. NMR studies of cyclohexene in solution[4] had reported the latter value to be 5.2 kcal/mol.

Acknowledgment. The authors thank the National Science Foundation and the Robert A. Welch Foundation for financial support.

(17) Bushweller, C. H.; O'Neil, J. W. *Tetrahedron Lett.* **1969**, 4713–4716.
(18) Larken, R. H.; Lord, R. C. *J. Am. Chem. Soc.* **1972**, *95*, 5129–5132.
(19) Camerlynek, R.; Anteunis, M. A. *Tetrahedron* **1975**, *31*, 1837–1840.
(20) Burkert, U.; Allinger, N. L. *Molecular Mechanics*; American Chemical Society: Washington, DC, 1982; ACS Monograph 177.

Ab Initio Vibrational Analysis of Hydrogen-Bonded *trans*- and *cis*-*N*-Methylacetamide

Noemi G. Mirkin and Samuel Krimm*

Contribution from the Biophysics Research Division and Department of Physics, University of Michigan, Ann Arbor, Michigan 48109. *Received April 15, 1991*

Abstract: In order to characterize the vibrational dynamics of the hydrogen-bonded *N*-methylacetamide (NMA) molecule, we have calculated the energies, geometries, and force constants (at the 4-31G* level) of *trans*-NMA and *cis*-NMA to which are hydrogen bonded two H_2O molecules, one at the NH group and one at the CO group. The force constants for *trans*-NMA were scaled to experimental frequencies for NMA in aqueous solution and resulted in predicted frequencies within 5 cm^{-1} of observed bands. Experimental data for *cis*-NMA are more limited, but transfer of scale factors from the isolated molecule permitted verification of the assignments of two resonance Raman bands proposed to be characteristic of this isomer.

The development of a reliable vibrational force field for the polypeptide chain is a prerequisite to the effective use of normal-mode analysis in rigorously correlating infrared and Raman spectra with structure of peptides and proteins. An extensive empirically refined force field has broken new ground in furthering this goal,[1] but such force fields are by their nature restricted and not unique. It is, therefore, natural to turn to ab initio methods to obtain the most comprehensive force fields for such analyses.

In the absence of ab initio calculations at the highest levels of basis set and electron correlation, which may not be feasible for large systems, it is necessary to scale the force constants in order to obtain agreement with experimental frequencies.[2] While generalized scale factors can give useful results, as we showed in the case of a study of conformers of dipeptides of glycine[3] and alanine,[4,5] a reliable set of force constants requires scaling to a relatively complete set of observed and assigned frequencies. The simplest protein-model peptide system for which this is possible

(1) Krimm, S.; Bandekar, J. *Adv. Protein Chem.* **1986**, *38*, 181–364.
(2) Fogarasi, G.; Pulay, P. In *Vibrational Spectra and Structure*; Durig, J. R., Ed.; Elsevier: New York, 1985; Vol. 14, pp. 125–219.
(3) Cheam, T. C.; Krimm, S. *J. Mol. Struct.* **1989**, *193*, 1–34.
(4) Cheam, T. C.; Krimm, S. *J. Mol. Struct. (Theochem)* **1989**, *188*, 15–43.
(5) Cheam, T. C.; Krimm, S. *J. Mol. Struct (Theochem)* **1990**, *206*, 173–203.

0002-7863/91/1513-9742$02.50/0

Table I. Relative and Binding Energies (kcal/mol) of Two Lowest Energy Conformers of Isolated and Hydrogen-Bonded *t*-NMA and *c*-NMA

conformer	isolated ΔE	hydrogen-bonded ΔE	hydrogen-bonded E_H
t-NMA (II)[a]	0	0.58	−13.45
t-NMA (IV)[a]	0.01	0	−14.04
c-NMA (I)[b]	0	0	−15.79
c-NMA (II)[b]	0.53	0.65	−15.67

[a] Reference 6. [b] Reference 7.

is *N*-methylacetamide (NMA), and we have presented such a force field for the isolated *trans*-NMA (*t*-NMA) molecule,[6] demonstrating in the process the sensitivity of the vibrational modes to the conformations of the methyl groups. We have also shown that these refined scale factors can, with minimum modification, account for the observed vibrational frequencies of the isolated *cis*-NMA (*c*-NMA) molecule.[7]

While such force fields are informative, they are not adequate to describe the hydrogen-bonded peptide group found in proteins. We have, therefore, thought it useful to obtain the scaled ab initio force fields of the *t*-NMA and *c*-NMA isomers in aqueous solution, systems that we have modeled by interacting NMA with two H_2O molecules, one at the CO group and the other at the NH group. Although the structure of water around the NMA molecule in solution is undoubtedly more complex, we believe that this simple model should nevertheless reveal the essential effects that hydrogen bonding has on the force constants and normal modes of the NMA molecule. As we have noted in a preliminary communication,[8] significant changes from the isolated molecule are indeed found.

Structures and Energies

Ab initio molecular orbital calculations were done at the Hartree–Fock level with the split valence basis set 4-31G* on *t*-NMA–$(H_2O)_2$ and *c*-NMA–$(H_2O)_2$. Although the 4-31G* basis set, which is quite large, still presents a small basis set superposition error,[9,10] we used it for the complexes because our earlier calculations for isolated NMA[6,7] were carried out at this level of theory. The reason for this is that we found that essentially the same frequencies and normal modes were obtained with 4-31G* as with 6-31G*. The calculations were carried out using GAUSSIAN 86[11] and GAUSSIAN 88[12] on an IBM 3090 and on a Cray Y-MP8/864 at the San Diego Supercomputer Center.

The starting geometries for NMA were the 4-31G* optimized geometries obtained for the isolated molecules.[6,7] The starting geometry for the H_2O molecules was also a 4-31G* optimized geometry. With respect to the positions of the H_2O molecules, the computation was carried out in two steps. In the first step, we started with the water positions reported by Jorgensen and Swenson[13] and Pullman et al.[14] and separately calculated the minimum energy structures first with one water molecule at the CO end and then with one at the NH end. Once we had these optimum positions at each end, we reoptimized the whole NMA–$(H_2O)_2$ complex with total relaxation of all the parameters.

Table II. Optimized 4-31G* Geometric Parameters of Isolated and Hydrogen-Bonded *t*-NMA and *c*-NMA

parameter[a]	*t*-NMA isolated	*t*-NMA H-bonded	*c*-NMA isolated	*c*-NMA H-bonded
CC	1.513	1.511	1.512	1.510
CO	1.199	1.209	1.198	1.213
CN	1.348	1.336	1.355	1.341
NH	0.992	0.996	0.995	1.000
NC	1.444	1.444	1.443	1.445
(N)CH[b]	1.081	1.081	1.080	1.080
(N)CH[c]	1.082	1.082	1.084	1.084
(C)CH[b]	1.083	1.081	1.079	1.078
(C)CH[c]	1.083	1.083	1.084	1.084
CCN	116.2	116.5	116.5	117.3
OCN	122.3	122.2	121.4	120.9
CNH	119.7	119.7	113.9	114.5
CNC	121.3	121.3	127.5	126.9
NCH[b]	108.7	108.5	108.2	107.9
NCH[c]	110.9	111.1	112.2	112.1
CCH[b]	113.7	113.0	108.2	109.3
CCH[c]	108.5	108.6	111.1	110.5
OCNH	180.0	180.0	0.0	0.0
OCNC	0.0	0.0	180.0	180.0
CCNH	0.0	0.0	180.0	180.0
CNCH[b]	180.0	180.0	180.0	180.0
CNCH[c]	60.2	60.2	61.2	61.2
CNCH[c]	−60.2	−60.2	−61.2	−61.2
NCCH[b]	0.0	0.0	180.0	180.0
NCCH[c]	−121.7	−122.0	−60.0	−59.6
NCCH[c]	121.7	122.0	60.0	59.6
OH		0.950		0.950
(O)HOH		105.1		105.9
(N)HOH		106.0		102.4
O···H_w		1.957		1.979
O···O_w		2.902		2.910
(N)H···O_w		2.089		2.135
N···O_w		3.085		3.045
CO···H_w		115.5		118.1
O···HO_w		172.5		165.9
NH···O_w		179.3		150.5

[a] Bond lengths in angstroms; bond angles in degrees. [b] In-plane H atoms. [c] Out-of-plane H atoms.

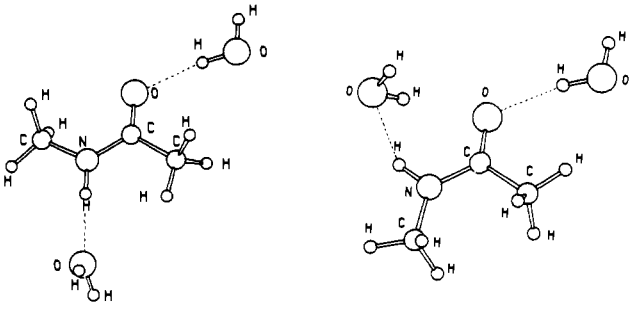

Figure 1. Optimized structures of *trans*-*N*-methylacetamide (left) and *cis*-*N*-methylacetamide (right) with two hydrogen-bonded water molecules.

In previous ab initio calculations of an amide–H_2O complex, the geometries of the monomers were held fixed and only the intermolecular geometrical parameters were optimized.[13-16]

Our previous ab initio studies of the conformers of isolated *t*-NMA and *c*-NMA indicated that the lowest energy structures at the 4-31G* level were structures II and IV for *t*-NMA[6] and structures I and II for *c*-NMA.[7] (The conformers are described by the relationship of a H atom on the adjoining CH_3 group to the (C)O and the (N)H. For *t*-NMA: I, cis–trans; II, cis–cis;

(6) Mirkin, N. G.; Krimm, S. *J. Mol. Struct.* **1991**, *242*, 143–160.
(7) Mirkin, N. G.; Krimm, S. *J. Mol. Struct.*, in press.
(8) Mirkin, N. G.; Krimm, S. *J. Am. Chem. Soc.* **1990**, *112*, 9016–9017.
(9) Hobza, P.; Sauer, J. *Theor. Chim. Acta* **1984**, *65*, 279–290.
(10) Dykstra, C. E. *Ab initio Calculations of the Structures and Properties of Molecules*; Elsevier: Amsterdam, 1988.
(11) Frisch, M. J.; Binkley, J. S.; Schlegel, H. B.; Raghavachari, K.; Melius, F. C.; Martin, R. L.; Stewart, J. J. P.; Bobrowicz, F. W.; Rohlfing, C. M.; Kahn, L. R.; DeFrees, D. J.; Seeger, R.; Whiteside, R. A.; Fox, D. J.; Fluder, E. M.; Pople, J. A. *GAUSSIAN 86*; Carnegie-Mellon Quantum Chemistry Publishing Unit: Pittsburgh, PA, 1984.
(12) Frisch, M. J.; Head-Gordon, M.; Schlegel, H. B.; Raghavachari, K.; Binkley, J. S.; Gonzalez, C.; DeFrees, D. J.; Fox, D. J.; Whiteside, R. A.; Seeger, R.; Melius, C. F.; Baker, J.; Martin, R. L.; Kahn, L. R.; Stewart, J. J. P.; Fluder, E. M.; Topiol, S.; Pople, J. A. *GAUSSIAN 88*; Gaussian,Inc.: Pittsburgh, PA, 1988.
(13) Jorgensen, W. L.; Swenson, C. J. *J. Am. Chem. Soc.* **1985**, *107*, 1489–1496.
(14) Pullman, A.; Alagona, G.; Tomasi, J. *Theor. Chim. Acta* **1974**, *33*, 87–90.
(15) Jorgensen, W. L.; Swenson, C. J. *J. Am. Chem. Soc.* **1985**, *107*, 569–578.
(16) Johansson, A.; Kollman, P.; Rothenberg, S.; McKelvey, J. *J. Am. Chem. Soc.* **1974**, *96*, 3794–3800.

III, trans–trans; IV, trans–cis. For *c*-NMA: I, cis–cis; II, cis–trans; III, trans–cis; IV, trans–trans.) The energy differences between these conformers were 0.01 and 0.53 kcal/mol for *t*-NMA and *c*-NMA, respectively. In order to see if these energy differences are maintained in the case of hydrogen bonding to the water molecules, we carried out the optimization procedure described above for all of these conformers.

The relative energies of the two conformers of each isomer for the isolated and hydrogen-bonded cases are given in Table I. The results show that, at this level of calculation, the order of stability and the difference in energy for *c*-NMA are maintained on hydrogen bonding, conformer I being lower in energy than conformer II. On the other hand, in the case of *t*-NMA, conformer IV with two H_2O molecules is lower in energy than conformer II and the energy difference for the hydrogen-bonded complexes is larger (0.58 kcal/mol) compared to the isolated molecules (0.01 kcal/mol). Table I also presents the binding energies E_H. These were calculated as the difference between the optimized energy of the NMA–$(H_2O)_2$ complex and the sum of the energies of the optimized isolated components.

Table II compares the optimized geometries for the isolated and hydrogen-bonded *t*- and *c*-NMA molecules (conformer IV for *t*-NMA and conformer I for *c*-NMA). These optimized structures are illustrated in Figure 1. In both isomers, the positions of the water molecule at the carbonyl end are such that the hydrogen not involved in the hydrogen bond points away from the *C*-methyl group. In *t*-NMA, the HOH bisector of the water molecule hydrogen bonded to the NH group makes an angle of 167.6° with the H···O direction; in *c*-NMA, the presence of the carbonyl oxygen reduces this angle to 86.0°. *trans*-NMA shows a linear hydrogen bond at the NH end with an H···O bond length of 2.089 Å. At the carbonyl end, the hydrogen bond is slightly nonlinear; the O···HO angle is 172.5°, and the O···H bond length is 1.957 Å. At this same end, the *c*-NMA isomer exhibits a hydrogen bond with a larger deviation from linearity, with the O···HO angle being 165.9° and a hydrogen bond length of 1.979 Å. At the NH end, the H···O bond length is 2.135 Å and the NH···O angle is 150.5°. This agrees with studies[17,18] which found that, in the special case of hydrates, when water is the proton donor, the hydrogen bonds tend to deviate considerably from linearity.

Vibrational Analysis

For the vibrational analysis, we considered only conformers IV and I for *t*- and *c*-NMA, respectively. The energy differences in Table I indicate that the concentrations of *t*-IV and *c*-I are about 3 times those of *t*-II and *c*-II, respectively, thus dominating the spectra. In any case, calculations for the latter two conformers show that in most cases the frequencies give comparable agreement with experiment; when the differences are large, the experimental data give preference to the lower energy conformers. The force constants for each complexed isomer were calculated by computing analytically the second derivatives of the 4-31G* energy at the optimized geometries. These force constants in Cartesian coordinates were then transformed into force constants in internal coordinates and scaled, and normal mode calculations were carried out using the Wilson GF method.[19] The internal and symmetry coordinates for the NMA portion of the hydrogen-bonded complexes are the same as those used previously.[6,7] Internal coordinates were defined for the H_2O molecules and hydrogen bonds, but their force constants and normal modes are not given here (unless they mix with NMA modes).

The scale factors defined for the different types of NMA internal coordinates are the same as those of ref 6. For *t*-NMA–$(H_2O)_2$, the direct transfer of scale factors that were optimized for the isolated molecule[6] yielded poor agreement with experimental Raman[20–23] and infrared[23] frequencies of aqueous NMA. With these scale factors, calculated frequencies that had contributions from coordinates involved in a hydrogen bond systematically deviated from the observed frequencies. Good agreement with experiment required the modification of scale factors corresponding to CN stretch (s), CO s, NC s, and CC s, CNH bend, and non-hydrogen in-plane deformations (d). These

Table III. Scale Factors for the Hydrogen-Bonded Complexes of *t*-NMA and *c*-NMA

internal coordinate	*t*-NMA–$(H_2O)_2$	*c*-NMA–$(H_2O)_2$
CN stretch	0.881	0.840
CO stretch	0.668	0.717
CC stretch and NC stretch	0.843	0.859
NH stretch	0.808	0.808
CH stretch	0.826	0.826
non-hydrogen in-plane deformations	0.911	0.998
CNH bend	0.761	0.763
NCH bend and CCH bend	0.782	0.782
HCH bend	0.778	0.778
out-of-plane bend and torsion	0.880	0.880

Table IV. Scaled Diagonal Force Constants of Isolated and Hydrogen-Bonded *t*-NMA and *c*-NMA

	value[b]			
	t-NMA		*c*-NMA	
force constant[a]	isolated[c]	hydrogen-bonded	isolated[d]	hydrogen-bonded
		A′ Modes[e]		
CN s	6.051	7.696	6.652	7.188
CO s	10.895	9.607	10.965	10.052
CC s	4.294	4.264	4.252	4.318
NC s	5.385	5.300	5.424	5.371
NH s	6.821	6.684	6.679	6.596
CCH_3 ss	4.955	4.976	4.959	4.975
CCH_3 as	4.820	4.876	4.920	4.956
NCH_3 ss	4.982	4.976	4.939	4.954
NCH_3 as	4.849	4.849	4.832	4.856
CCN d	1.290	1.194	1.378	1.480
CO ib	1.384	1.281	1.464	1.662
CNC d	0.857	0.814	0.905	1.017
NH ib	0.503	0.537	0.490	0.719
CCH_3 sb	0.537	0.546	0.528	0.544
CCH_3 r	0.604	0.628	0.609	0.646
CCH_3 ab	0.516	0.511	0.520	0.515
NCH_3 sb	0.607	0.605	0.601	0.604
NCH_3 r	0.761	0.761	0.776	0.781
NCH_3 ab	0.541	0.542	0.560	0.560
		A″ Modes[e]		
CCH_3 as	4.848	4.851	4.766	4.781
NCH_3 as	4.804	4.787	4.709	4.727
CCH_3 r	0.566	0.573	0.529	0.542
CCH_3 ab	0.516	0.518	0.519	0.524
NCH_3 r	0.768	0.765	0.766	0.765
NCH_3 ab	0.530	0.532	0.540	0.541
CO ob	0.807	0.823	0.843	0.853
NH ob	0.052	0.084	0.061	0.094
CN t	0.328	0.377	0.272	0.307
CC t	0.002	0.023	0.044	0.040
NC t	0.013	0.018	0.023	0.027

[a] Key: s = stretch, ss = symmetric stretch, as = antisymmetric stretch, sb = symmetric bend, ab = antisymmetric bend, ib = in-plane bend, ob = out-of-plane bend, r = rock, d = deformation, t = torsion. [b] Units: Mdyn Å^{-1}, for stretch constants; mdyn Å, for all others. [c] From ref 6. [d] From ref 7. [e] Key: A′, in-plane; A″, out-of-plane.

(17) Olovsson, I.; Jönsson, P. In *The Hydrogen Bond*; Shuster, P., Zundel, G.; Sandorfy, C., Eds.; North-Holland Publishing: Amsterdam, 1976; Vol. II.
(18) Del Bene, J. *Struct. Chem.* **1988**, *1*, 19–27.
(19) Wilson, E. B., Jr.; Decius, J. C.; Cross, P. C. *Molecular Vibrations*; McGraw-Hill: New York, 1955.
(20) Mayne, L. C.; Ziegler, L. D.; Hudson, B. *J. Phys. Chem.* **1985**, *89*, 3395–3398.
(21) Dudik, J. M.; Johnson, C. R.; Asher, S. A. *J. Phys. Chem.* **1985**, *89*, 3805–3814.
(22) Wang, Y.; Purrello, R.; Spiro, T. G. *J. Am. Chem. Soc.* **1989**, *111*, 8274–8276.
(23) Song, S.; Asher, S. A.; Krimm, S.; Shaw, K. D. *J. Am. Chem. Soc.* **1991**, *113*, 1155–1163.

scale factors were optimized by a least-squares fitting of the calculated to the observed frequencies. The experimental data on aqueous *c*-NMA[22,23] are much more limited than on *t*-NMA, and we therefore intended to make only the minimal changes in scale factors needed to give agreement with clearly assignable cis bands. As it happened, this required no changes in scale factors from those of the isolated molecule.[7] Table III presents the resulting scale factors for the two hydrogen-bonded complexes.

The scaled diagonal force constants for each isolated and hydrogen-bonded isomer are shown on Table IV. The off-diagonal force constants ≥0.03 for the hydrogen-bonded structures are given in Table VIII (supplementary material). Tables V and VI present the calculated NMA frequencies for the isolated and hydrogen-bonded cases of *t*- and *c*-NMA, respectively, and compare these with experimental data for matrix-isolated[24] and aqueous NMA.[20-23] As in the case of the isolated molecules,[6,7] the CH_3 torsion (t) coordinates were excluded from the calculation, since this part of the potential surface is poorly described at this level of basis set. Because of the simplicity of the aqueous *t*-NMA spectrum, and the detailed ab initio analysis of the isolated molecule,[6] assignments for the hydrogen-bonded molecule were straightforward and presented no problems.

Discussion

The absolute energy difference between *t*-NMA-$(H_2O)_2$ and *c*-NMA-$(H_2O)_2$ is found to be 0.69 kcal/mol. At this level of theory, the trans conformation is also the most stable on hydrogen bonding, but the relative energy has decreased considerably (down from 2.44 kcal/mol[7]). Of course, this energy difference refers only to the $(H_2O)_2$ structure and not to more realistic $(H_2O)_n$ complexes that exist in aqueous solution.

Table I shows the binding energies E_H for the conformers of both *t*- and *c*-NMA. These values are for the two hydrogen bonds involved in each complex, and they show that the combined hydrogen bonds are stronger in the cis conformers by about 2 kcal/mol. When we optimize NMA with only one water molecule at a time, we find that for the *c*-NMA complex the two hydrogen bonds (at the NH and CO ends) have similar strengths, −8.7 and −7.6 kcal/mol. On the other hand, for the *t*-NMA-H_2O complex the hydrogen bond at the NH end is weaker than the one at the carbonyl end, viz., −5.4 vs −8.7 kcal/mol. These results are in agreement with those of amide-H_2O complexes reported by Pullman and co-workers for calculations with minimal basis sets[14] and by Jorgensen et al. for calculations with the 3-21G and 6-31G* basis sets.[13,15] Therefore, the difference of ~2 kcal/mol in the hydrogen-bond binding energies between the two isomers is due to the difference in the strengths of the hydrogen bond at the NH end. At this end, a water molecule binds more weakly in *t*-NMA than in *c*-NMA. This may seem strange since the H···O distance at the NH end is longer in *c*-NMA than in *t*-NMA (2.135 vs 2.089 Å). However, because the hydrogen bond is not linear in this case, the N···O distance is shorter in *c*-NMA than in *t*-NMA (3.045 vs 3.085 Å).

The hydrogen-bond strengths can be correlated with the Mulliken electron populations on the (N)H atom in the isolated molecule: The smaller the population, the stronger the hydrogen bond formed.[16] Table VII shows the Mulliken electron populations for the isolated and hydrogen-bonded *t*- and *c*-NMA. We see that the population on (N)H of isolated *c*-NMA (0.618) is indeed smaller than that in *t*-NMA (0.627), consistent with the proposed relation[16] and with our results. In general, the charge differences for each atom between isolated *t*-NMA and *c*-NMA are mostly less than 0.02e. On hydrogen bonding, however, the negative charge on N increases by slightly more than this, 0.032e and 0.021e for *t*-NMA and *c*-NMA, respectively, the negative charge on O increases by much more, 0.043e and 0.045e, respectively, and the negative charge on (N)H decreases significantly, 0.072e and 0.042e, respectively. The atomic populations of the methyl groups remain fairly constant for both isomers.

(24) Ataka, S.; Takeuchi, H.; Tasumi, M. *J. Mol. Struct.* **1984**, *113*, 147-160.

Table V. Observed and Calculated Frequencies (cm^{-1}) of Isolated and Hydrogen-Bonded *t*-NMA

ν(obs)[a]	ν(calc)	potential energy distribution[b]
		A′ Modes[c]
3498	3510	NH s (100)
	3460	NH s (101)
3008	3002	CCH_3 as (100)
	3010	CCH_3 as (101)
2978	2992	NCH_3 as (100)
	3002	NCH_3 as (101)
2958	2932	NCH_3 ss (100)
	2935	CCH_3 ss (100)
2915	2928	CCH_3 ss (99)
	2930	NCH_3 ss (100)
1708	1700	CO s (83), CCN d (11)
1622	1623	CO s (73), CCN d (12), CN s (11)
1511	1512	NH ib (44), CN s (33)
1580	1585	NH ib (45), CN s (45)
1472	1469	NCH_3 ab (79)
	1468	NCH_3 ab (83), NCH_3 r (10)
1446	1441	CCH_3 ab (70), CCH_3 sb (10)
1435	1444	CCH_3 ab (60), CCH_3 sb (18)
1419	1423	NCH_3 sb (96)
1418	1421	NCH_3 sb (92)
1370	1378	CCH_3 sb (80), CCH_3 ab (14)
1380	1382	CCH_3 sb (63), CCH_3 ab (25)
1265	1266	NH ib (26), CO ib (19), CN s (15), CCH_3 sb (10)
1315	1306	NH ib (29), CCH_3 sb (19), CN s (18), CO ib (11)
1181	1179	NCH_3 r (38), NC s (14)
1167	1173	NCH_3 r (51), NC s (13)
1089	1096	NC s (54), NCH_3 r (13)
1097	1098	NC s (52), CCH_3 r (13)
990	984	CCH_3 r (53), CC s (20)
999	994	CCH_3 r (58), CC s (15), NC s (10)
857	861	CN s (32), NCH_3 r (21), CNC d (10)
886	879	NCH_3 r (22), CN s (18), CC s (15)
658	649	CC s (37), CO ib (33)
633	638	CO ib (35), CC s (34)
439	450	CCN d (51), CO ib (30), CCH_3 r (15)
446	444	CCN d (53), CO ib (30), CCH_3 r (12)
279	280	CNC d (66), CCN d (34)
	284	CNC d (60), CCN d (27)
		A″ Modes[c]
3008	2997	NCH_3 as (101)
	2997	CCH_3 as (101)
2973	2990	CCH_3 as (100)
	2984	NCH_3 as (100)
1446	1441	NCH_3 ab (94)
	1443	NCH_3 ab (94)
1432	1429	CCH_3 ab (92)
1435	1436	CCH_3 ab (91)
	1117	NCH_3 r (91)
	1119	NCH_3 r (91)
1037	1053	CCH_3 r (59), CO ob (21)
1046	1059	CCH_3 r (59), CO ob (22)
626	639	CO ob (68), CCH_3 r (30)
	607	CO ob (64), CCH_3 r (27), NH ob (20), NH···O ob (18)
391	401	CN t (103), NH ob (68), CO ob (20)
	697	CN t (38), NH···O ob (33), CO ob (16), NH ob (13)
	168	NH ob (60), CN t (14)
	174	NH ob (39), CN t (36)

[a] Key: top line, matrix-isolated;[24] bottom line, aqueous solution.[20-23] [b] Key: s = stretch, ss = symmetric stretch, as = antisymmetric stretch, sb = symmetric bend, ab = antisymmetric bend, ib = in-plane bend, ob = out-of-plane bend, r = rock, d = deformation, t = torsion. Contributions ≥10. [c] Key: A′, in-plane; A″, out-of-plane.

As for the geometries, several structural changes are seen in NMA on hydrogen bonding (Table II). The CO and NH bond

Table VI. Observed and Calculated Frequencies (cm^{-1}) of Isolated and Hydrogen-Bonded *c*-NMA

ν(obs)[a]	ν(calc)	potential energy distribution[b]
		A′ Modes[c]
3458	3471	NH s (100)
	3409	NH s (100)
	3031	CCH_3 as (93)
	3045	CCH_3 as (92)
	3001	NCH_3 as (93)
	3009	NCH_3 as (93)
	2923	CCH_3 ss (86)
	2926	CCH_3 ss (82)
	2914	NCH_3 ss (86)
	2918	NCH_3 ss (83)
1707	1717	CO s (78), CCN d (12)
	1702	HOH b (49), CO s (26)
~1650	1645	HOH b (50), CO s (28)
1485	1481	NCH_3 ab (54), CN s (16), NCH_3 r (14)
1496	1499	CN s (33), CC s (11), NCH_3 ab (10)
1454	1465	NCH_3 sb (41), NCH_3 ab (25), CN s (17)
	1471	NCH_3 ab (36), NCH_3 sb (30), NH ib (11)
	1438	NH ib (34), NCH_3 sb (27), NC s (16), NCH_3 ab (14)
	1459	NCH_3 ab (43), NH ib (24), CCH_3 ab (10)
1432	1424	CCH_3 ab (77), NCH_3 sb (18)
	1424	CCH_3 ab (72), NCH_3 sb (14)
1387	1392	CCH_3 sb (44), NH ib (21), NCH_3 sb (13)
	1411	NCH_3 sb (39), CCH_3 sb (28), NH ib (10)
1325	1331	CCH_3 sb (51), CN s (17), NH ib (12), CO ib (12)
	1354	CCH_3 sb (63), CN s (11)
	1204	NC s (40), NCH_3 r (30)
	1203	NC s (44), NCH_3 r (30)
1075	1083	NCH_3 r (31), NC s (21), CCH_3 r (15), NH ib (12)
	1097	NCH_3 r (36), NC s (19), CCH_3 r (15)
	983	CCH_3 r (52), NCH_3 r (16)
	998	CCH_3 r (58), NCH_3 r (14)
	798	CC s (52), CN s (20), NC s (10)
821	808	CC s (58), CN s (20), NC s (11)
607	596	CO ib (28), NC s (17), CCN d (12), CC s (10)
	612	CO ib (46), NC s (16), CC s (12), CN s (11)
510	523	CCN d (43), CO ib (41), CNC d (26), CCH_3 r (23)
	557	CCN d (39), CO ib (22), CNC d (22), CCH_3 r (12)
	294	CNC d (53), CCN d (33)
	308	CNC d (55), CCN d (34)
		A″ Modes[c]
	2973	CCH_3 as (95)
	2976	CCH_3 as (95)
	2959	NCH_3 as (95)
	2966	NCH_3 as (94)
	1453	NCH_3 ab (73), CCH_3 ab (21)
	1456	NCH_3 ab (70), CCH_3 ab (23)
	1437	CCH_3 ab (72), NCH_3 ab (22)
	1440	CCH_3 ab (71), NCH_3 ab (23)
	1114	NCH_3 r (92)
	1114	NCH_3 r (92)
	1047	CCH_3 r (60), CO ob (23)
	1056	CCH_3 r (65), CO ob (30)
	516	CN t (36), CO ob (26), NH ob (17), CCH_3 r (13)
	678	CN t (33), CO ob (29), NH ob (21), CCH_3 r (13)
	634	CO ob (53), CCH_3 r (26), CN t (12), NH ob (11)
	552	CO ob (43), CN t (20), NH ob (19), CCH_3 r (15)
	112	NH ob (116), CN t (85), CO ob (16)
	128	CN t (38), NH ob (22)

[a] Key: top line, matrix-isolated;[24] bottom line, aqueous solution.[20-23] [b] Key: s = stretch, ss = symmetric stretch, as = antisymmetric stretch, sb = symmetric bend, ab = antisymmetric bend, ib = in-plane bend, ob = out-of-plane bend, r = rock, d = deformation, t = torsion. Contributions ≥10. [c] Key: A′, in-plane; A″, out-of-plane.

lengths increase substantially, while the CN bond decreases by 0.012 Å in *t*-NMA and 0.014 Å in *c*-NMA. The former changes are consistent with hydrogen-bond formation, while the latter changes suggest an increase in double-bond character of the CN bond on hydrogen bonding. As expected, the methyl group bond lengths and angles are not affected by the addition of the water molecules.

Table VII. Mulliken Electron Populations for *t*-NMA and *c*-NMA

	t-NMA		*c*-NMA	
atom	isolated	hydrogen-bonded	isolated	hydrogen-bonded
N	7.783	7.815	7.777	7.798
H	0.627	0.555	0.618	0.576
C	5.254	5.243	5.258	5.234
O	8.617	8.660	8.613	8.658
(N)C	6.257	6.259	6.266	6.271
H^a	0.839	0.836	0.816	0.808
H^b	0.814	0.820	0.828	0.825
(C)C	6.559	6.578	6.576	6.592
H^a	0.798	0.791	0.785	0.753
H^b	0.841	0.829	0.818	0.813

[a] In-plane H. [b] Out-of-plane H.

As expected, some diagonal force constants (Table IV) experience major changes when NMA is hydrogen bonded to two water molecules. We discuss these changes in detail only for *t*-NMA, for which there are good data and reliable assignments for both isolated and hydrogen-bonded molecules and therefore we can have reasonable confidence in the scale factors. The largest change in the diagonal force constants (~60%) occurs for NH out-of-plane bend (ob) (we discuss below the basis for its scale factor). The CO s force constant decreases by about 12% while the NH s force constant exhibits a 2% decrease. This agrees with the results of Cheam and Krimm,[25] in that the decreases in the NH s and CO s harmonic force constants on hydrogen bonding are due primarily to increases in the lengths of the NH and CO bonds. The CN s force constant increases by 27%, again consistent with its shorter bond length, which also explains the increase in the CN t force constant. The 7% increase in the NH in-plane bend (ib) force constant seems to be a natural result of hydrogen bonding, but the 7% decrease in CO ib does not fit this pattern (obviously, other changes in electronic structure dominate over the effect of hydrogen bonding). Other skeletal deformation force constants (CCN d and CNC d) show a 6–8% decrease. Not surprisingly, CH_3 group force constants are not appreciably affected by hydrogen bonding. The changes in *c*-NMA force constants show similar trends; exact descriptions must await reliable scale factors. With respect to off-diagonal force constants (Table VIII, supplementary material), hydrogen bonding produces significant changes in their magnitudes as well as the signs. As expected, the largest changes are in interaction force constants that involve NH, CO, and CN bonds.

Since some force constants are altered by hydrogen bonding, we naturally expect frequencies to change. It should, of course, not be surprising that normal modes are also affected. For *t*-NMA (Table V), amide I is lowered (from 1700 to 1623 cm^{-1}) and gains a small CN s component; amide II increases (from 1512 to 1585 cm^{-1}) and shows a small relative increase in CN s; amide III also increases (from 1266 to 1306 cm^{-1}) and the relative proportions of CO ib and CCH_3 sb change; and amide V undergoes a large predicted increase (from 401 to 697 cm^{-1}) with a very significant change in its normal mode. In this connection, we have not scaled the latter mode to the supposed observed amide V band at 748 cm^{-1} in aqueous NMA[26] for two reasons. First, it has proven to be difficult to reproduce this band (Shaw, K. D., Krimm, S. Private communication), undoubtedly because of the strong interference by water in this region. Second, maintaining the ob scale factor at 0.880[6] leads to a reasonable reproduction of the observed 9-cm^{-1} increase in the ~1040-cm^{-1} CCH_3 r, CO ob mode (the predicted increase is 10 cm^{-1} if we take the calculated frequency of the preferred conformer II of the isolated molecule[6]). Of course, the

(25) Cheam, T. C.; Krimm, S. *J. Mol. Struct.* **1986**, *146*, 175–189.
(26) Song, S.; Asher, S. A.; Krimm, S.; Bandekar, J. *J. Am. Chem. Soc.* **1988**, *110*, 8547–8548.

scale factor for NH ob and CN t might be different from that for CO ob; additional experimental data will be needed to test this point. We note that this scale factor cannot be fixed by an assignment of the observed 633-cm^{-1} band to the CO ob mode now calculated at 607 cm^{-1}; the latter contains NH ob, and our experimental results indicate that the 633-cm^{-1} band is unshifted in D_2O, confirming its assignment to the CO ib mode.

For *c*-NMA (Table VI), analogous changes are seen, although we can be less certain about details because of the paucity of data, which led us to maintain the scale factors of the isolated molecule. These nevertheless reproduce quite well the amide II like mode observed at 1496 cm^{-1} [22,23] and show that there is a significant change in its character on hydrogen bonding. The amide I mode interacts strongly with HOH bend, a result of the near-coincidence in frequencies for the current value of the CO s scale factor; additional data will be needed to verify this prediction. Amide III is predicted to increase (from 1331 to 1354 cm^{-1}), but this band has not been observed. The presence of a *cis* band at 821 cm^{-1}, well separated from the similar *trans* band at 886 cm^{-1}, is clearly seen[23] and is reasonably well reproduced by the calculation.

Conclusions

In order to examine the effect that hydrogen bonding has on the frequencies and normal modes of NMA, we have compared the *ab initio* force constants, frequencies, and modes of isolated *t*-NMA and *c*-NMA with those of a model system in which the NH and CO groups are each hydrogen bonded to a water molecule. While such an NMA-$(H_2O)_2$ model cannot realistically represent the water structure surrounding the NMA molecule in aqueous solution, it should provide an appropriate description of the characteristic changes that hydrogen bonding produces in the vibrational dynamics of the NMA molecule.

For *t*-NMA-$(H_2O)_2$, calculations at the 4-31G* level (which provided satisfactory scaled force constants and vibrational modes for the isolated molecule[6]) together with readily assigned observed bands led to optimized scale factors that resulted in good agreement between observed and calculated frequencies (the average discrepancy for observed bands below 1700 cm^{-1} is 5.1 cm^{-1}). The expected increases in bond lengths on hydrogen bonding are found for the NH and CO bonds. The accompanying shortening of the CN bond indicates that its double-bond character increases on hydrogen bonding. Associated changes in force constants correlate well with these geometric changes and with other expected effects of hydrogen bonding.

The calculated *c*-NMA-$(H_2O)_2$ results are more difficult to scale because of the limited experimental data on this molecule in aqueous solution. Transfer of scale factors without change from the isolated molecule[7] could nevertheless confirm the assignments of a new band at 1496 cm^{-1} in high-energy-pulsed resonance Raman spectra to the amide II like mode of *c*-NMA[22,23] and a new band at 821 cm^{-1} to this isomer as well.[23] While trends in force constant changes on hydrogen bonding are generally similar to those in *t*-NMA, more reliable values will have to await optimization of scale factors based on more extensive data.

Acknowledgment. This research was supported by National Science Foundation Grants DMB-8816756 and DMR-8806975.

Supplementary Material Available: Table giving scaled off-diagonal force constants of hydrogen-bonded *t*-NMA and *c*-NMA (3 pages). Ordering information is given on any current masthead page.

Vibrational Circular Dichroism and Absolute Configuration of Substituted Thiiranes

Prasad L. Polavarapu,*,† Simeon T. Pickard,† Howard E. Smith,*,† Thomas M. Black,† Arvi Rauk,*,‡ and Danya Yang‡

Contribution from the Departments of Chemistry, Vanderbilt University, Nashville, Tennessee 37235, and University of Calgary, Calgary, Alberta, Canada T2N 1N4.
Received April 22, 1991

Abstract: Experimental vibrational circular dichroism (VCD) spectra for *trans*-2,3-dimethylthiirane and its *2,3-d_2* isotopomer were measured in the 1600-700-cm^{-1} region. Ab initio theoretical calculations of VCD using the localized molecular orbital formalism were carried out with the 6-31G* basis set. Similar calculations were also done using the vibronic coupling formalism for *trans*-2,3-dimethylthiirane, its *2,3-d_2* isotopomer, and methylthiirane. A comparison between the theoretical model predictions and the experimental data reveals that the theoretical models are successful in reproducing the experimental VCD spectra. The merits and limitations of the individual models are discussed.

Introduction

Vibrational circular dichroism (VCD) is anticipated to provide new approaches to the determination of three-dimensional structure of chiral molecules in isotropic media. Experimental techniques[1-6] have developed to the extent that reliable spectra can be obtained anywhere from the near-infrared region to the long-wavelength side of the mid-infrared region (~700 cm^{-1}). At the same time, three different quantum-theoretical methods became available[7-15] for predicting the VCD spectra. One of the current active research areas involves testing these theoretical methods for their predictive capability. Small chiral molecules which can be subjected to a rigorous theoretical vibrational analysis are crucial for this purpose. For this reason, recent theoretical evaluations were focused on 2,3-dideuteriooxirane,[15-17] 1,2-di-

† Vanderbilt University.
‡ University of Calgary.

(1) (a) Holzwarth, G.; Hsu, E. C.; Mosher, H. S.; Faulkner, T. R.; Moscowitz, A. *J. Am. Chem. Soc.* **1974**, *96*, 251-252. (b) Nafie, L. A.; Keiderling, T. A.; Stephens, P. J. *J. Am. Chem. Soc.* **1976**, *98*, 2715-2723.
(2) Cianciosi, S. J.; Ragunathan, N.; Freedman, T. B.; Nafie, L. A.; Baldwin, J. E. *J. Am. Chem. Soc.* **1990**, *112*, 8204-8206.
(3) Narayanan, U.; Keiderling, T. A.; Elsevier, C. J.; Vermeer, P.; Runge, W. *J. Am. Chem. Soc.* **1988**, *110*, 4133-4138.
(4) Diem, M.; Roberts, G. M.; Lee, O.; Barlow, A. *Appl. Spectrosc.* **1988**, *42*, 20-26.
(5) For a collection of references on the subject, see: Polavarapu, P. L. In *Vibrational Spectra and Structure*, Bist, H. D., Durig, J. R., Sullivan, J. F., Eds.; Elsevier: New York, 1989; Vol. 17B, pp 319-342.
(6) Polavarapu, P. L. *Appl. Spectrosc.* **1989**, *43*, 1295-1297.
(7) Walnut, T. W.; Nafie, L. A. *J. Chem. Phys.* **1977**, *67*, 1501-1510.
(8) Nafie, L. A.; Walnut, T. W. *Chem. Phys. Lett.* **1977**, *49*, 441-446.

0002-7863/91/1513-9747$02.50/0